J|A|C|S
ARTICLES

Anionic Snieckus−Fries Rearrangement: Solvent Effects and Role of Mixed Aggregates

Jason C. Riggs, Kanwal J. Singh, Ma Yun, and David B. Collum*

Department of Chemistry and Chemical Biology, Baker Laboratory, Cornell University, Ithaca, New York 14853-1301

Received May 30, 2008; E-mail: dbc6@cornell.edu

Abstract: Lithiated aryl carbamates (ArLi) bearing methoxy or fluoro substituents in the meta position are generated from lithium diisopropylamide (LDA) in THF, *n*-BuOMe, Me_2NEt, dimethoxyethane (DME), *N,N,N′,N′*-tetramethylethylenediamine (TMEDA), *N,N,N′,N′*-tetramethylcyclohexanediamine (TMCDA), and hexamethylphosphoramide (HMPA). The aryllithiums are shown with ^6Li, ^{13}C, and ^{15}N NMR spectroscopies to be monomers, ArLi−LDA mixed dimers, and ArLi−LDA mixed trimers, depending on the choice of solvent. Subsequent Snieckus−Fries rearrangements afford ArOLi−LDA mixed dimers and trimers of the resulting phenolates. Rate studies of the rearrangement implicate mechanisms based on monomers, mixed dimers, and mixed trimers.

Introduction

The anionic Snieckus−Fries rearrangement of aryl carbamates (eq 1a) is a highly effective means of carrying out ortho substitutions.[1,2] Its popularity stems in large part from the dogged determination of Snieckus and co-workers to optimize the protocol and expand the scope of the reaction (which prompts us to cast a vote for adding Snieckus to the name).[3−6]

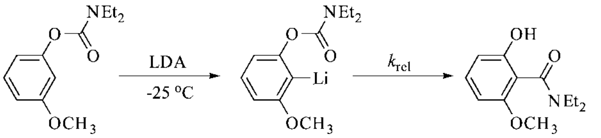

(1)

Table 1a

solvent[3]	yield	k_{rel}
THF	88	5
THF/HMPA	84	7700
n-BuOMe	83	1
DME	94	90
TMCDA	87	90
TMEDA	83	12
Me_2NEt	88	2

Our interest in the Snieckus−Fries rearrangement was piqued by its probative value to study organolithium structure−reactivity relationships. Dimethylcarbamates bearing no meta substituent favor rapid intramolecular acyl transfer, affording insight into only the slow (rate-limiting) ortholithiation step.[7] By contrast, aryl carbamates bearing activating meta substituents (OCH_3 or F) and bulky carbamoyl groups rapidly form a relatively stable intermediate aryllithium, allowing the rearrangement step to be examined as well.[8]

The consistently high yields accompanying eq 1a suggest that the choice of coordinating solvent is unimportant, but yields offer little insight into reactivity.[9] The relative rate constants (k_{rel}) show that the choice of coordinating solvent markedly influences the rate of acyl transfer. Of course, solvent-dependent relative reactivities do not offer direct insights into underlying organolithium structures and reaction mechanisms.[10,11]

In a previous study we investigated reactivities and mechanisms of the ortholithiation of aryl carbamates, paying only limited attention to the acyl transfer.[7] This paper focuses

---

(1) (a) Hartung, C. G.; Snieckus, V. In *Modern Arene Chemistry*; Astruc, D., Ed.; Wiley-VCH: Weinheim, 2002; Chapter 10. (b) Snieckus, V. *Chem. Rev.* **1990**, *90*, 879. (c) Taylor, C. M.; Watson, A. J. *Curr. Org. Chem.* **2004**, *8*, 623.

(2) Sibi, M. P.; Snieckus, V. *J. Org. Chem.* **1983**, *48*, 1935.

(3) LDA = lithium diisopropylamide (LDA); DME = 1,2-dimethoxyethane; TMEDA = *N,N,N′N′*-tetramethylethylenediamine; TMCDA = *trans-N,N,N′,N′*-tetramethylcyclohexanediamine (optically pure *R,R* or *S,S* enantiomer); and HMPA = hexamethylphosphoramide.

(4) (a) The Lewis acid-mediated version was discovered by Fries in 1908[5a] A photochemical variant was first described in 1960,[5b] and the anionic variant appears to have been first reported by Melvin in 1981.[5c] Snieckus reported the first anionic Fries rearrangement of an aryl carbamate in 1983.[2]

(5) (a) Fries, K.; Finck, G. *Ber.* **1908**, *41*, 2447. (b) Anderson, J. C.; Reese, C. B. *Proc. Chem. Soc.* **1960**, 217. (c) Melvin, L. S. *Tetrahedron Lett.* **1981**, 3375.

(6) Industrial applications:(a) Nguyen, T.; Wicki, M. A.; Snieckus, V. *J. Org. Chem.* **2004**, *69*, 7816. (b) Mhaske, S. B.; Argade, N. P. *J. Org. Chem.* **2004**, *69*, 4563. (c) Harfenist, M.; Joseph, D. M.; Spence, S. C.; Mcgee, D. P. C.; Reeves, M. D.; White, H. L. *J. Med. Chem.* **1997**, *40*, 2466. (d) Piettre, A.; Chevenier, E.; Massardier, C.; Gimbert, Y.; Greene, A. E. *Org. Lett.* **2002**, *4*, 3139. (e) Dankwardt, J. W. *J. Org. Chem.* **1998**, *63*, 3753. (f) Mohri, S.; Stefinovic, M.; Snieckus, V. *J. Org. Chem.* **1997**, *62*, 7072. (g) Lampe, J. W.; Hughes, P. F.; Biggers, C. K.; Smith, S. H.; Hu, H. *J. Org. Chem.* **1994**, *59*, 5147. (h) Ding, F.; Zhang, Y.; Qu, B.; Li, G.; Farina, V.; Lu, B. Z.; Senanayake, C. H. *Org. Lett.* **2008**, *10*, 1067.

(7) (a) Singh, K. J.; Collum, D. B. *J. Am. Chem. Soc.* **2006**, *128*, 13753. (b) Ma, Y.; Collum, D. B. *J. Am. Chem. Soc.* **2007**, *129*, 14818.

(8) (a) Kauch, M.; Hoppe, D. *Can. J. Chem.* **2001**, *79*, 1736. (b) Kauch, M.; Snieckus, V.; Hoppe, D. *J. Org. Chem.* **2005**, *70*, 7149.

(9) Collum, D. B. *Acc. Chem. Res.* **1992**, *25*, 448.

(10) (a) Bernstein, M. P.; Collum, D. B. *J. Am. Chem. Soc.* **1993**, *115*, 8008. (b) Sun, X.; Collum, D. B. *J. Am. Chem. Soc.* **2000**, *122*, 2452. (c) Zhao, P.; Collum, D. B. *J. Am. Chem. Soc.* **2003**, *125*, 14411.

(11) Collum, D. B.; McNeil, A. J.; Ramirez, A. *Angew. Chem., Int. Ed.* **2007**, *46*, 3002.

10.1021/ja804087r CCC: $40.75

exclusively on the acyl transfer. We describe herein studies of solvent-dependent structures of the intermediate lithiated aryl carbamates and evidence of monomer-, mixed dimer-, and mixed trimer-based mechanisms for the rearrangement.[12] The mixed *trimer*-based pathway may represent the first documented example of an organolithium reaction in which the rate-limiting transition structure is *more* highly aggregated than the reactants.[13]

Results

A series of structural, kinetic, and computational studies are described below. The choice of substrates was not as arbitrary as it might seem. Rate studies demand structural homogeneity to maximize the clarity of the results.[11,14] The wide range of solvent-dependent reactivities foreshadowed by eq 1a demanded tinkering with the carbamoyl group and meta substituent to optimize the protocol for characterizing the starting aryllithiums and monitoring the rearrangements. General descriptions of protocols are followed by specific results organized according to solvent.

Structural Studies. Lithium diisopropylamide (LDA), [^{6}Li]-LDA, and [^{6}Li,^{15}N]LDA were prepared as white crystalline solids.[15,16] Previous investigations of LDA solvated by THF, *n*-BuOMe, THF/HMPA, and Me$_2$NEt have revealed dimers **1a--d** as the sole observable forms.[3,17a,d] Bifunctional ligands DME and TMEDA afford nonchelated dimers **2a** and **2b**, respectively.[3,17b,c] LDA solvated by TMCDA forms exclusively monomer **3**.[3,17b]

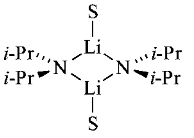

1a; S = THF
1b; S = *n*-BuOMe
1c; S = HMPA
1d; S = Me$_2$NEt

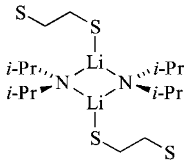

2a; S = OMe (DME)
2b; S = NMe$_2$ (TMEDA)

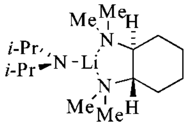

3

Aryllithiums **6a–g**, mixed dimers **7a–h**, and mixed trimers **8a–b** were generated from aryl carbamates **4a–e**[18] using [^{6}Li]LDA or [^{6}Li,^{15}N]LDA. Rearrangement in the presence of excess LDA affords phenolate-based mixed dimers **9a–d** and mixed trimers **10a–e**, which were synthesized independently by lithiating phenols **5a–c** with excess [^{6}Li,^{15}N]LDA.

Table 1. ^{6}Li and ^{15}N NMR Spectroscopic Data[a,b]

ArLi	solvent	R	X	^{6}Li, δ (mult, $^1J_{\mathrm{LiN}}$)	^{15}N, δ(mult)
6a[c]	THF	*i*-Pr	F	1.23 (s)	–
6c[b]	HMPA	*i*-Pr	OMe	0.91 (s)	–
6e	HMPA	*i*-Pr	F	0.75 (s)	–
6f[c,b]	DME	*i*-Pr	F	1.65 (s)	–
6g[b]	TMCDA	Et	OMe	2.18 (s)	–
7b[b]	THF	*i*-Pr	F	1.71 (d, 5.3)	76.3 (q)
7d[b]	*n*-BuOMe	Et	OMe	1.85 (d, 5.8)	75.8 (q)
7f[b]	DME	*i*-Pr	F	1.60 (d, 5.4)	75.2 (q)
7g	TMEDA	*i*-Pr	OMe	2.01 (d, 4.9)	75.3 (q)
7h	Me$_2$NEt	Et	OMe	1.93 (d,5.2)	75.3 (q)
8a	TMEDA	*i*-Pr	OMe	0.78 (d, 5.7) 2.49 (t, 4.7) 2.50 (d, 5.7)	73.8 (tt) 75.3 (q)
8b	Me$_2$NEt	Et	OMe	0.81 (d, 6.3) 2.24 (d, 6.0)2.80 (t, 4.9)	74.2 (tt) 74.3 (q)
9a	THF	Me	F	0.40 (d, 4.8)	79.1 (q)
9b	*n*-BuOMe	Et	OMe	0.93 (d, 4.9)	75.1 (q)
9c	HMPA	Et	OMe	0.54 (d, 5.3)	76.5 (q)
9d	HMPA	Me	F	0.66 (d, 4.6)	76.3 (q)
10a	*n*-BuOMe	Et	OMe	1.49 (d, 5.5) 1.55 (d, 6.2) 1.89 (t, 5.2)	74.4 (–)[d] 74.1 (–)[d]
10b	HMPA	Et	OMe	1.09 (d, 5.3) 1.12 (d, 5.3) 1.58 (t, 4.6)	73.2 (–)[d] 74.7 (tt)
10c	DME	Me	F	0.95 (d, 4.7) 0.98 (d, 5.1) 1.82 (t, 5.1)	72.9 (q) 74.3 (q)
10d	TMEDA	Me	OMe	1.21 (d, 5.0) 1.67 (t, 4.9)	74.9 (q) 75.1 (q)
10e	Me$_2$NEt	Et	OMe	1.79 (d, 6.2) 1.79 (t, 5.1) 1.84 (d, 6.1)	73.8 (tt) 74.3 (tt)

[a] Multiplicities are denoted as follows: s, singlet; d, doublet; t, triplet; q, quintet. The chemical shifts are reported relative to 0.30 M ^{6}LiCl/MeOH (δ 0.0 ppm) and neat Me$_2$NEt (δ 25.7 ppm) at −90 °C. ^{13}C NMR spectra are referenced to toluene-d_8 (δ 137.9 ppm), pentane (δ 14.1 ppm), or THF (δ 67.6 ppm). Chemical shifts are reported in ppm, and J values are reported in Hz. [b] Carbon-13 resonances of the carbanionic carbons: **6c**, δ 158.7 (br s); **6f**, δ 150.1 (br d, $J_{\mathrm{FC}} = 120.7$); **6g**, δ 155.1 (t, $J_{\mathrm{CLi}} = 7.7$); **7b**, δ 150.5 (br d, $J_{\mathrm{FC}} = 123$); **7d**, δ 155.2 (q, $J_{\mathrm{CLi}} = 5.7$); **7f**, δ 154.6 (dq, $J_{\mathrm{FC}} = 123$, $J_{\mathrm{CLi}} = 5.9$). [c] 1.0 equiv [^{6}Li,^{15}N]LDA. [d] Obscured by another resonance.

The structural assignments stem from splitting patterns observed using one-dimensional ^{6}Li, ^{15}N, and ^{13}C NMR spectroscopies[17a] as well as ^1J(^{6}Li,^{15}N)-resolved[19] and ^{6}Li,^{15}N-HSQC NMR spectroscopies.[20] Spectroscopic data are summarized in Table 1, and spectra are archived in Supporting Information. Although the structures and affiliated equilibria are complex, the methods used are well established. In lieu of detailed descriptions of the assignments for each solvent–substrate–aggregate combination, a few general statements should suffice.

(1) Some monomeric aryllithiums could be generated only by using 1.0 equiv of [^{6}Li,^{15}N]LDA in some cases (**6a** and **6f**), whereas other monomers are formed even with excess [^{6}Li,^{15}N]LDA (**6b–e** and **6g**). The anticipated ^{6}Li–^{13}C coupling is seen by ^{13}C NMR spectroscopy in some cases, but most show only broad mounds. We have noted, however, that mixtures of such putative aryllithium monomers do not form ArLi–Ar′Li heteroaggregates,[21] consistent with the monomer assignment.[22] Previous spectroscopic studies strongly support a prevalence

---

(12) For leading references and discussions of mixed aggregation effects, see: (a) Seebach, D. *Angew. Chem., Int. Ed. Engl.* **1988**, *27*, 1624. (b) Tchoubar, B.; Loupy, A. *Salt Effects in Organic and Organometallic Chemistry*; VCH: New York, 1992; Chapters 4, 5, and 7. (c) Briggs, T. F.; Winemiller, M. D.; Xiang, B.;.; Collum, D. B. *J. Org. Chem.* **2001**, *66*, 6291. (d) Caubere, P. *Chem. Rev.* **1993**, *93*, 2317. (e) Gossage, R. A.; Jastrzebski, J. T. B. H.; van Koten, G. *Angew. Chem., Int. Ed* **2005**, *44*, 1448. (f) Seebach, D. In *Proceedings of the Robert A. Welch Foundation Conferences on Chemistry and Biochemistry*; Wiley: New York, 1984; p 93,

(13) The exchange of free and bound TMEDA on a TMEDA-chelated lithium amide monomer appears to proceed by dimer-based mechanism: Lucht, B. L.; Bernstein, M. P.; Remenar, J. F.; Collum, D. B. *J. Am. Chem. Soc.* **1996**, *118*, 10707.

(14) The rate law provides the stoichiometry of the transition structure relative to that of the reactants: Edwards, J. O.; Greene, E. F.; Ross, J. *J. Chem. Educ.* **1968**, *45*, 381.

(15) Kim, Y.-J.; Bernstein, M. P.; Galiano-Roth, A. S.; Romesberg, F. E.; Fuller, D. J.; Harrison, A. T.; Collum, D. B.; Williard, P. G. *J. Org. Chem.* **1991**, *56*, 4435.

(16) The spins of ^{6}Li, ^{13}C, and ^{15}N are 1, 1/2, and 1/2, respectively.

(17) (a) Collum, D. B. *Acc. Chem. Res.* **1993**, *26*, 227. (b) Remenar, J. F.; Lucht, B. L.; Collum, D. B. *J. Am. Chem. Soc.* **1997**, *119*, 5567. (c) Bernstein, M. P.; Romesberg, F. E.; Fuller, D. J.; Harrison, A. T.; Williard, P. G.; Liu, Q. Y.; Collum, D. B. *J. Am. Chem. Soc.* **1992**, *114*, 5100. (d) Romesberg, F. E.; Gilchrist, J. H.; Harrison, A. T.; Fuller, D. J.; Collum, D. B. *J. Am. Chem. Soc.* **1991**, *113*, 5751.

(18) (a) Lustig, E.; Benson, W. R.; Duy, N. *J. Org. Chem.* **1967**, *32*, 851. (b) Yamagami, C.; Takao, N.; Nishioka, T.; Fujita, T.; Takeuchi, Y. *Org. Magn. Reson.* **1984**, *22*, 439.

(19) Rutherford, J. L.; Collum, D. B. *J. Am. Chem. Soc.* **1999**, *121*, 10198.

(20) Xiang, B.; Winemiller, M. D.; Briggs, T. F.; Fuller, D. J.; Collum, D. B. *Magn. Reson. Chem.* **2001**, *39*, 137.

Table 2. Summary of Rate Studies for the Anionic Snieckus–Fries Rearrangement

ArLi	solvent	R	X	temperature °C	LDA Order	solvent order
7a	THF	Me	F	−40	0, −0.48 ± 0.04	1.08 ± 0.05,[a] 2.4 ± 0.6[b]
7d	*n*-BuOMe	Et	OMe	15	0,[c] 0.49 ± 0.09[d]	0, −1.10 ± 0.05
6b[e]	HMPA	Et	OMe	−65	0	0.8 ± 0.1
6d[e]	HMPA	Me	F	−78	0	1.2 ± 0.3
7e	DME	Me	F	−60	0	0
6g	TMCDA	Et	OMe	−25	0	0

[a] 0.42 M LDA. [b] 0.098 M LDA. [c] 7.0 M *n*-BuOMe. [d] 1.3 M *n*-BuOMe. [e] The order in THF cosolvent is zero.

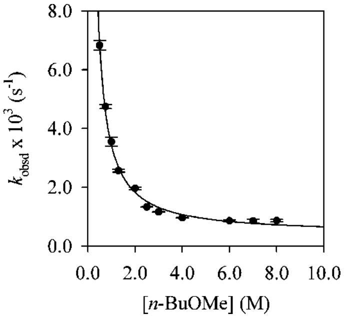

Figure 1. Plot of k_{obsd} vs [*n*-BuOMe] in pentane cosolvent for the rearrangement of **7d** (0.004 M) by LDA (0.075 M) at 15 °C. The curve depicts an unweighted least-squares fit to $k_{obsd} = k[n\text{-BuOMe}]^n + k'$ ($k = (3.0 \pm 0.1) \times 10^{-3}$, $n = -1.10 \pm 0.05$, $k' = (4.1 \pm 0.1) \times 10^{-4}$).

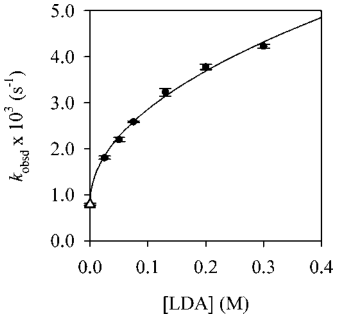

Figure 2. Plot of k_{obsd} vs [LDA] in 1.3 M *n*-BuOMe/pentane for the rearrangement of **7d** (0.004 M) at 15 °C. The curve depicts an unweighted least-squares fit to $k_{obsd} = k[\text{LDA}]^n + k'$ ($k = (6.3 \pm 0.2) \times 10^{-3}$, $n = 0.49 \pm 0.09$, $k' = (7.9 \pm 0.2) \times 10^{-4}$). k' (see ●) was set to equal k' in Figure 3.

of monomers.[23−25] Especially large $^2J_{FC}$ couplings (>100 Hz) in the ^{13}C NMR spectra are similar to those observed in other orthofluorinated aryllithiums.[7,23a,b,26]

(2) Mixed dimers (**7**) available by using excess [^{6}Li,^{15}N]LDA show characteristic ^{6}Li doublets and ^{15}N quintets consistent with the $Li_a-N_b-Li_c$ connectivity. The asymmetry imparted by chelation of the carbamate moiety could be observed as two ^{6}Li resonances at very low temperature (<−125 °C). ^{13}C NMR spectra show quintets due to coupling of the lithiated carbon to two ^{6}Li nuclei and, in the case of the meta fluoro species, are further split by J_{FC} coupling.

(3) Mixed trimers (**8**) display three ^{6}Li resonances in a 1:1:1 ratio, manifesting the ^{6}Li−^{15}N coupling consistent with a $Li_a-N_b-Li_c-N_d-Li_e$ subunit. Each mixed trimer also displays a triplet of triplets and a quintet in the ^{15}N NMR spectrum. The asymmetry confirms the chelation of the carbamate moiety as drawn.

(4) Phenolate mixed dimers (**9**) display characteristic ^{6}Li doublets and ^{15}N quintets that are consistent with $Li_a-N_b-Li_c$ connectivity. The ^{6}Li resonances of the phenolate mixed dimers are upfield from the aryllithium mixed dimers (**7**).

(5) Phenolate mixed trimers (**10**) show three ^{6}Li resonances as two doublets and one triplet in a 1:1:1 ratio. Two ^{15}N resonances appear as either triplet of triplets or quintets.[7,27]

Rate Studies. General Methods.[11,28,29] The anionic Snieckus–Fries rearrangement was monitored using an in situ IR spectrometer fitted with a 30-bounce, silicon-tipped probe.[30] The

---

(21) Singh, K. J.; Hoepker, A. C.; Collum, D. B. Cornell University, Ithaca, NY. Unpublished work.

(22) For a discussion and leading references to the use of mixed aggregation to provide insight into homoaggregation, see ref 47b.

(23) (a) Ramirez, A.; Candler, J.; Bashore, C. G.; Wirtz, M. C.; Coe, J. W.; Collum, D. B. *J. Am. Chem. Soc.* **2004**, *126*, 14700. (b) Riggs, J. C.; Ramirez, A.; Cremeens, M. E.; Bashore, C. G.; Candler, J.; Wirtz, M. C.; Coe, J. W.; Collum, D. B. *J. Am. Chem. Soc.* **2008**, *130*, 3406. (c) Stratakis, M.; Wang, P. G.; Streitwieser, A. *J. Org. Chem.* **1996**, *61*, 3145. (d) Reich, H. J.; Green, D. P.; Medina, M. A.; Goldenberg, W. S.; Gudmundsson, B.Ö.; Dykstra, R. R.; Phillips, N. H. *J. Am. Chem. Soc.* **1998**, *120*, 7201.

(24) (a) Crittendon, R. C.; Beck, B. C.; Su, J.; Li, X. W.; Robinson, G. H. *Organometallics* **1999**, *18*, 156. (b) Olmstead, M. M.; Power, P. P. *J. Organomet. Chem.* **1999**, *408*, 1. (c) Girolami, G. S.; Riehl, M. E.; Suslick, K. S.; Wilson, S. R. *Organometallics* **1992**, *11*, 3907. (d) Bosold, F.; Zulauf, P.; Marsch, M.; Harms, K.; Lohrenz, J.; Boche, G. *Angew. Chem., Int. Ed.* **1991**, *30*, 1455. (e) Hardman, N. J.; Twamley, B.; Stender, M.; Baldwin, R.; Hino, S.; Schiemenz, B.; Kauzlarich, S. M.; Power, P. P. *J. Organomet. Chem.* **2002**, *643*, 461. (f) Wegner, G. L.; Berger, R. J. F.; Schier, A.; Schmidbaur, H. *Z. Naturforsch., B: Chem. Sci.* **2000**, *55*, 995. (g) Schiemenz, B.; Power, P. P. *Angew. Chem., Int. Ed.* **1996**, *35*, 2150. (h) Maetzke, T.; Seebach, D. *Helv. Chim. Acta* **1989**, *72*, 624. (i) Kottke, T.; Sung, K.; Lagow, R. J. *Angew. Chem., Int. Ed. Engl.* **1995**, *34*, 1517.

(25) For representative computational studies of aryllithiums, see: (a) Krasovsky, A.; Straub, B. F.; Knochel, P. *Angew. Chem., Int. Ed.* **2006**, *45*, 159. (b) Bachrach, S. M.; Chamberlin, A. C. *J. Org. Chem.* **2004**, *69*, 2111. (c) Kwon, O.; Sevin, F.; McKee, M. L. *J. Phys. Chem. A* **2001**, *105*, 913. (d) Wiberg, K. B.; Sklenak, S.; Bailey, W. F. *J. Org. Chem.* **2000**, *65*, 2014. (e) Kremer, T.; Junge, M.; Schleyer, P. v. R. *Organometallics* **1996**, *15*, 3345. (f) Also, see ref 23b.

(26) (a) Menzel, K.; Fisher, E. L.; DiMichele, L.; Frantz, D. E.; Nelson, T. D.; Kress, M. H. *J. Org. Chem.* **2006**, *71*, 2188. (b)$^2J_{C\text{-}F}$ values have been correlated with π-bond orders and total electronic charge at the ^{13}C atom: Doddrell, D.; Barfield, M.; Adcock, W.; Aurangzeb, M.; Jordan, D. *J. Chem. Soc., Perkin Trans.* **1976**, *2*, 402.

(27) (a) The homoaggregated phenolates tend to be insoluble, and their often complex structures in solution are unknown. Structurally analogous lithium phenolates bearing carbonyl-containing moieties in the ortho position have been characterized crystallographically: Wang, Z.; Chai, Z.; Li, Y. *J. Organomet. Chem.* **2005**, *690*, 4252. (b) Boyle, T. J.; Pedrotty, D. M.; Alam, T. M.; Vick, S. C.; Rodriguez, M. A. *Inorg. Chem.* **2000**, *39*, 5133. (c) Clegg, W.; Lamb, E.; Liddle, S. T.; Snaith, R.; Wheatley, A. E. H. *J. Organomet. Chem.* **1999**, *573*, 305. (d) Cetinkaya, B.; Gumrukcu, I.; Lappert, M. F.; Atwood, J. L.; Shakir, R. *J. Am. Chem. Soc.* **1980**, *102*, 2086. (e) Khanjin, N. A.; Menger, F. M. *J. Org. Chem.* **1997**, *62*, 8923.

(28) (a) Hsieh, H. L.; Quirk, R. P. *Anionic Polymerization: Principles and Practical Applications*; Marcel Dekker: New York, 1996. (b) Wardell, J. L. In *Comprehensive Organometallic Chemistry*; Wilkinson, G.; Stone, F. G. A., Abel, E. W., Eds.; Pergamon: New York, 1982; Vol. 1, Chapter 2. (c) Szwarc, M., Ed. *Ions and Ion Pairs in Organic Reactions*; Wiley: New York, 1972; Vol. I, II.

(29) Espenson, J. H. *Chemical Kinetics and Reaction Mechanisms*, 2nd ed.; McGraw-Hill: New York, 1995.

(30) Rein, A. J.; Donahue, S. M.; Pavlosky, M. A. *Curr. Opin. Drug Discov. Dev.* **2000**, *3*, 734.

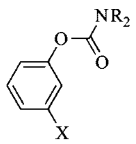

4a; R= Me, X = OMe
4b; R = Et, X = OMe
4c; R = *i*-Pr, X = OMe
4d; R = Me, X = F
4e; R= *i*-Pr, X= F

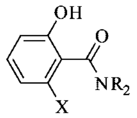

5a; R = Me, X = OMe
5b; R = Et, X = OMe
5c; R = Me, X = F

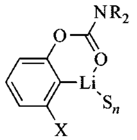

6a; S = THF, R = *i*-Pr, X = F
6b; S = HMPA, R = Et, X = OMe
6c; S = HMPA, R = *i*-Pr, X = OMe
6d; S = HMPA, R = Me, X = F
6e; S = HMPA, R = *i*-Pr, X = F
6f; S = DME, R = *i*-Pr, X = F
6g; S = η^2-TMCDA, R = Et, X = OMe

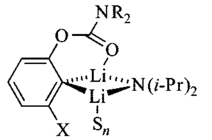

7a; S = THF, R = Me, X = F
7b; S = THF, R = *i*-Pr, X = F
7c; S = *n*-BuOMe, R = Me, X = F
7d; S = *n*-BuOMe, R = Et, X = OMe
7e; S = DME, R = Me, X = F
7f; S = DME, R= *i*-Pr, X= F
7g; S = η^1-TMEDA, R = *i*-Pr, X = OMe
7h; S = Me_2NEt, R = Et, X = OMe

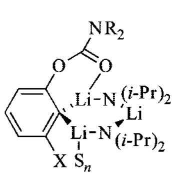

8a; S = η^1-TMEDA, R = *i*-Pr, X = OMe
8b; S = Me_2NEt, R = Et, X = OMe

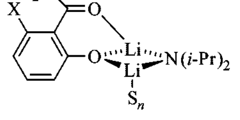

9a; S = THF, R = Me, X = F
9b; S = *n*-BuOMe, R = Et, X = OMe
9c; S = HMPA, R = Et, X = OMe
9d; S = HMPA, R = Me, X = F

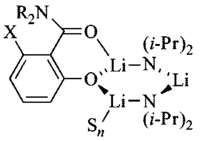

10a; S = *n*-BuOMe, R = Et, X = OMe
10b; S = HMPA, R = Et, X = OMe
10c; S = DME, R = Me, X = F
10d; S = η^1-TMEDA, R = Me, X = OMe
10e; S = Me_2NEt, R = Et, X = OMe

carbonyl group provided an excellent handle for following the loss of the aryllithium (monomer **6** or mixed dimer **7**; 1670−1690 cm^{-1}) and the growth of the aryl carboxamide (**9** or **10**; 1590−1610 cm^{-1}). Pseudo-first-order conditions were established by maintaining the aryllithium concentration at 0.004 M. Mixed dimers **7a**, **7d**, and **7e** and monomers **6b**, **6d**, and **6g** were generated in situ with excess LDA. Solvent concentrations were high, yet adjustable, using a cosolvent (pentane, hexane, or toluene).[31] The resulting pseudo-first-order rate constants (k_{obsd}) are independent of the initial concentration of the aryllithium, confirming a first-order dependence. The decays also follow first-order dependencies, as shown by least-squares fits to the nonlinear Noyes equation.[32] Phenolate-based mixed aggregates **9** and **10** or any unforeseen conversion-dependent changes were shown to be inconsequential under the pseudo-first-order conditions by reestablishing the baseline at the end of a run, injecting a second aliquot of aryl carbamate, and confirming that the first and second rate constants are equivalent (±10%). The reaction orders are summarized in Table 2.

Computations. Calculations based on density functional theory (DFT) were performed at the B3LYP/6-31G(d) level of theory using Gaussian 03 and visualized with GaussView 3.09.[33] Gibbs free energies ($\Delta G°$, kcal/mol) include thermal corrections at 298 K. Calculated transition structures were shown to be legitimate saddle points by the existence of a single imaginary frequency. The alkyl groups on the carbamate were modeled as methyl groups, and LDA was modeled as lithium dimethylamide. THF and *n*-BuOMe were modeled as dimethylether (Me_2O). TMCDA was modeled as TMEDA. The results, comprising 43 calculated reactants and 23 calculated transition structures, are archived in Supporting Information. Selected observations are presented in the context of the specific solvents as described below.

THF. The metalation of **4d** and subsequent rearrangement in THF solution were studied previously;[7] the results are summarized to provide context. Rearrangement of mixed dimer **7a** in THF and excess LDA affords LDA−lithium phenolate mixed dimer **9a**. The idealized rate law[34] for the rearrangement (eq 2) is consistent with parallel pathways via transition structures **11** and **12** (eq 4). Computations using Me_2NLi/Me_2O suggest that **7a** is a monosolvated mixed dimer as drawn, and they support **11** and **12** implicated by the rate law.

$$-d[\mathbf{7a}]/dt = k'[\mathbf{7a}][THF]^1[LDA]^0 + k''[\mathbf{7a}][THF]^2[LDA]^{-1/2} \quad (2)$$

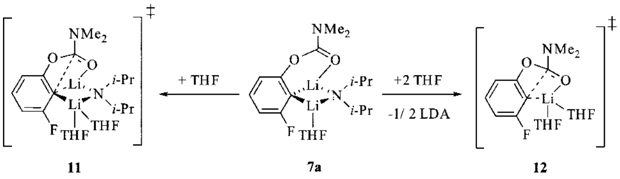

(3)

***n*-BuOMe.** Lithiation of **4b** with excess LDA/*n*-BuOMe affords mixed dimer **7d** as the only observable form. Solvation numbers cannot be ascertained spectroscopically, but DFT computations (see Supporting Information) suggest that monosolvated mixed dimer **7d** is favored. Rearrangement of **7d** in *n*-BuOMe with excess LDA affords LDA−lithium phenolate mixed dimer **9b** and mixed trimer **10a**.

A plot of k_{obsd} vs *n*-BuOMe concentration (Figure 1) for the rearrangement of mixed dimer **7d** reveals two limiting behaviors: (1) an *inverse* dependence on *n*-BuOMe concentration, which is consistent with a mechanism requiring solvent dissociation, and (2) a zeroth-order dependence on *n*-BuOMe concentration, indicating a nondissociative mechanism. Plots of k_{obsd} vs LDA concentration (Figures 2 and 3) show a *positive* half-order LDA dependence with a nonzero intercept at low *n*-BuOMe concentration (affiliated with the mechanism requiring solvent dissociation) and a zeroth-order LDA dependence at high *n*-BuOMe concentration (affiliated with the nondissociative mechanism). The reaction orders are consistent with the idealized rate law in eq 4, the mechanisms described generically in eqs 5−7, and

---

(31) The concentration of the LDA, although expressed in units of molarity, refers to the concentration of the monomer unit (normality). The concentrations of solvent are expressed as total concentration of free (uncoordinated) form.

(32) Briggs, T. F.; Winemiller, M. D.; Collum, D. B.; Parsons, R. L., Jr.; Davulcu, A. K.; Harris, G. D.; Fortunak, J. D.; Confalone, P. N. *J. Am. Chem. Soc.* **2004**, *126*, 5427.

(33) (a) Frisch, M. J.; et al. *Gaussian 03*, revision B.04; Gaussian, Inc.: Wallingford, CT, 2004. (b) Dennington, R., II; Keith, T.; Millam, J.; Eppinnett, K.; Hovell, W. L.; Gilliland, R. *GaussView*, Version 3.09; Semichem, Inc.: Shawnee Mission, KS, 2003.

(34) We define the idealized rate law as that obtained by rounding the observed reaction orders to the nearest rational order.

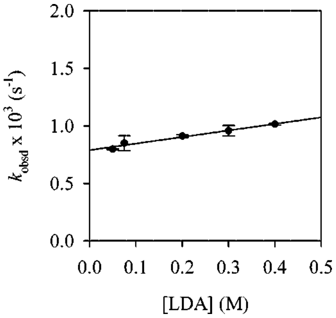

Figure 3. Plot of k_{obsd} vs [LDA] in 7.0 M *n*-BuOMe/pentane for the rearrangement of **7d** (0.004 M) at 15 °C. The curve depicts an unweighted least-squares fit to $k_{obsd} = k[\text{LDA}] + k'$ ($k = (5.7 \pm 0.8) \times 10^{-4}$, $k' = (7.9 \pm 0.2) \times 10^{-4}$).

transition structures **13** and **14** (eq 1). Although mixed dimer **7d** is the observable form, the Snieckus−Fries rearrangement is *faster* via mixed *trimer*-based transition structure **13**. Calculations using Me$_2$NLi/Me$_2$O support both **13** and **14** as viable and suggest a greater preference for **13** (although such a non-isodesmic comparison should be made with caution if at all).

$$-\mathrm{d}[\mathbf{7d}]/\mathrm{d}t = k'[\mathbf{7d}][n\text{-BuOMe}]^{-1}[\text{LDA}]^{1/2} + k''[\mathbf{7d}][n\text{-BuOMe}]^{0}[\text{LDA}]^{0} \quad (4)$$

$$\underset{(\mathbf{7d})}{(i\text{-Pr}_2\text{NLi})(\text{ArLi})(n\text{-BuOMe})} + 1/2(i\text{-Pr}_2\text{NLi})_2(n\text{-BuOMe})_2 \rightleftarrows (i\text{-Pr}_2\text{NLi})_2(\text{ArLi})(n\text{-BuOMe}) + (n\text{-BuOMe}) \quad (5)$$

$$(i\text{-Pr}_2\text{NLi})_2(\text{ArLi})(n\text{-BuOMe}) \rightarrow \underset{(\mathbf{13})}{[(i\text{-Pr}_2\text{NLi})_2(\text{ArLi})(n\text{-BuOMe})]^{\ddagger}} \quad (6)$$

$$\underset{(\mathbf{7d})}{(i\text{-Pr}_2\text{NLi})(\text{ArLi})(n\text{-BuOMe})} \rightarrow \underset{(\mathbf{14})}{[(i\text{-Pr}_2\text{NLi})(\text{ArLi})(n\text{-BuOMe})]^{\ddagger}} \quad (7)$$

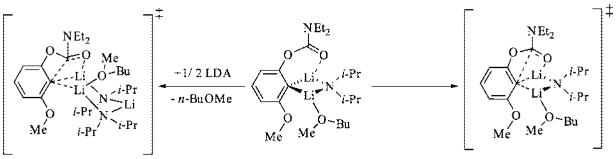

(8)

13 **7d** **14**

HMPA. Metalation of **4c** and **4e** with LDA/HMPA/THF affords monomers **6c** and **6e** to the exclusion of mixed aggregates even with excess LDA.[35] Unfortunately, $^1J_{\text{CLi}}$ coupling was not observed in the ^{13}C NMR spectra. ^{6}Li−^{31}P coupling was also absent.[36] Rearrangement of **6b** in HMPA/THF and excess LDA affords LDA−lithium phenolate mixed dimer **9c** and mixed trimer **10b**. By contrast, rearrangement of **6d** in HMPA/THF and excess LDA affords only LDA−lithium phenolate mixed dimer **9d**.

A plot of k_{obsd} vs HMPA concentration (Figure 4) for the rearrangement of monomer **6b** reveals a first-order dependence on HMPA concentration (with a relatively minor nonzero intercept) consistent with a dominant mechanism requiring solvation by one additional HMPA. Plots of k_{obsd} vs LDA concentration and k_{obsd} vs THF concentration reveal zeroth-order dependencies. The idealized rate law (eq 9) is consistent with the mechanisms described generically in eq 10 and transition structure **15**. Analogous results are obtained using the fluorinated aryllithium monomer **6d**, albeit at approximately 3-fold slower rearrangement rates, presumably due to inductive stabilization. Similar relative reactivities of MeO- and F-substituted aryllithiums were observed for the elimination of lithium halides to form benzynes.[23b]

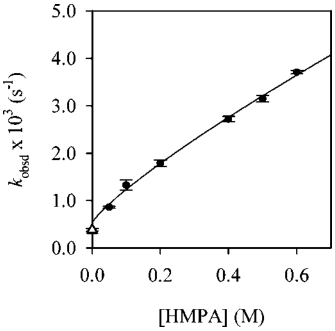

Figure 4. Plot of k_{obsd} vs [HMPA] in 10.0 M THF/hexanes cosolvent for the rearrangement of **6b** (0.004 M) by LDA (0.10 M) at −65 °C. The curve depicts an unweighted least-squares fit to $k_{obsd} = k[\text{HMPA}]^n + k'$ ($k = (4.8 \pm 0.2) \times 10^{-3}$, $n = 0.8 \pm 0.1$, $k' = (0.5 \pm 0.2) \times 10^{-3}$). Pseudo-first-order conditions not maintained at 0.05 M HMPA (△); data was omitted from the fit.

$$-\mathrm{d}[\mathbf{6b}]/\mathrm{d}t = k'[\mathbf{6b}][\text{HMPA}]^{1}[\text{THF}]^{0}[\text{LDA}]^{0} \quad (9)$$

$$\underset{(\mathbf{6b})}{(\text{ArLi})(\text{HMPA})_n} + \text{HMPA} \rightarrow \underset{(\mathbf{15})}{[(\text{ArLi})(\text{HMPA})_{n+1}]^{\ddagger}} \quad (10)$$

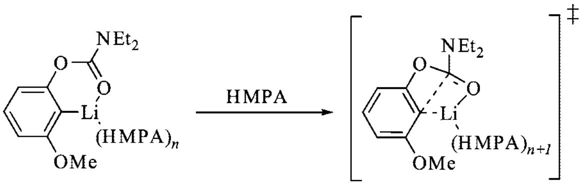

(11)

6b **15**

DME. Lithiation of **4e** with excess LDA/DME affords mixed dimer **7f** as the sole observable aggregate. Unlike *n*-BuOMe, DME can be η^1- or η^2-coordinated in either the reactant or the transition structure. DFT computations indicate that (1) the substitution of *n*-BuOMe by η^1-coordinated DME is nearly thermoneutral (eq 12), and (2) the η^2-coordinated mixed dimer (**18**) is 5.1 kcal/mol favored over the η^1-coordinated mixed dimer **17** (eq 13). One Li−C bond of η^2-coordinated mixed dimer **18** is long (2.88 Å) with an accompanying shortening of the Li−F contact, however, suggesting cleavage (ring expansion) to accommodate the second oxygen of DME. Although the calculations are provocative, the veracity of **18** is undermined by experimental binding studies (discussed below). The open dimer motif of **18**, however, resurfaces in the context of the rate studies described below.

Plots of k_{obsd} vs DME concentration and k_{obsd} vs LDA concentration for the rearrangement of mixed dimer **7e** reveal that the rearrangement is *independent* of both the DME and LDA concentrations. The reaction orders are consistent with

---

(35) Romesberg, F. E.; Collum, D. B. *J. Am. Chem. Soc.* **1994**, *116*, 9198.

(36) (a) Reich, H. J.; Kulicke, K. J. *J. Am. Chem. Soc.* **1995**, *117*, 6621. (b) Reich, H. J.; Green, D. P.; Medina, M. A.; Goldenberg, W. J.; Gudmundsson, B. Ö.; Dykstra, R. R.; Philips, N. H. *J. Am. Chem. Soc.* **1998**, *120*, 7201. (c) Reich, H. J.; Sikorski, W. H.; Gudmundsson, B. Ö.; Dykstra, R. R. *J. Am. Chem. Soc.* **1998**, *120*, 4035. (d) Reich, H. J.; Holladay, J. A.; Mason, J. D.; Sikorski, W. H. *J. Am. Chem. Soc.* **1995**, *117*, 12137. (e) Reich, H. J.; Borst, J. P.; Dykstra, R. R.; Green, D. P. *J. Am. Chem. Soc.* **1993**, *115*, 8728. (f) Jantzi, K. L.; Puckett, C. L.; Guzei, I. A.; Reich, H. J. *J. Org. Chem.* **2005**, *70*, 7520.

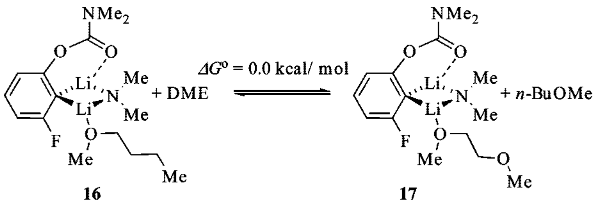

(12)

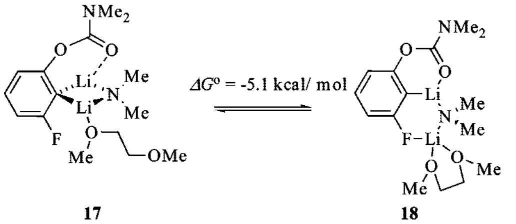

(13)

the idealized rate law in eq 14, the mechanism described generically in eq 15, and transition structure **19**. Notably, the reaction is much faster (approximately *90 times* in eq 1a) than it is in neat *n*-BuOMe. The origins of the acceleration are instructive about the role of chelation in the reactant **7e** and transition structure **19**.

$$-\mathrm{d}[\mathbf{7e}]/\mathrm{d}t = k'[\mathbf{7e}][\mathrm{DME}]^0[\mathrm{LDA}]^0 \qquad (14)$$

$$\underset{(\mathbf{7e})}{(i\text{-Pr}_2\mathrm{NLi})(\mathrm{ArLi})(\mathrm{DME})} \rightarrow \underset{(\mathbf{19})}{[(i\text{-Pr}_2\mathrm{NLi})(\mathrm{ArLi})(\mathrm{DME})]^{\ddagger}} \qquad (15)$$

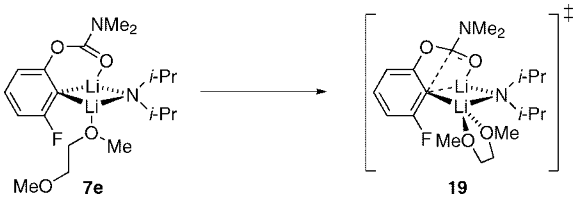

(16)

To understand the binding of DME in mixed dimer **7e** we experimentally measured the relative binding energies of *n*-BuOMe and DME using a variation of a Job plot as follows.[37] The rearrangement was carried out in DME/*n*-BuOMe mixtures according to Scheme 1. The total concentration of DME and *n*-BuOMe is held fixed at 5.0 M. The proportion is expressed as a mole fraction of DME, *X*. The observed rate constant is described as a function of the mole fraction according to eq 17. Three possible limiting results are illustrated in Figure 5. If *n*-BuOMe and DME bind equivalently ($K_{eq} = 1$), a plot of k_{obsd} vs mole fraction of DME will be linear. If chelation causes DME to be a superior ligand ($K_{eq} = 10$), then the rate will rise and saturate at relatively low DME concentrations. In the unlikely event that *n*-BuOMe is superior to DME as a ligand for the mixed dimer ($K_{eq} = 0.1$), then the opposite curvature will be observed.

$$k_{obsd} = [k_{BuOMe} + (k_{DME}K_{eq} - k_{BuOMe})X_{DME}]/[1 + (K_{eq} - 1)X_{DME}] \qquad (17)$$

Scheme 1

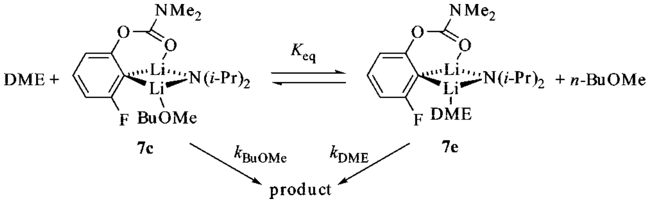

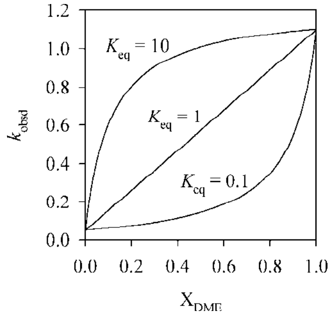

Figure 5. Theoretical curves describing k_{obsd} vs mole fraction of DME (X_{DME}) according to eq 17 for mixtures of *n*-BuOMe and DME. The assumed values of K_{eq} are as labeled. The relative rate constants for k_{BuOMe} and k_{DME} correspond to the left and right *y*-intercepts and arbitrarily assigned as 0.05 and 1.1, respectively.

The data in Figure 6 shows curvature consistent with slight preference for solvation by DME compared to *n*-BuOMe ($\Delta G° = -0.2$ kcal/mol). Therefore, either η^2-coordinated DME is not present, or the η^1 and η^2 forms are isoenergetic. For the sake of further discussion, we depict **7e** as containing unchelated DME as drawn. Although it is unclear why the computations (cf. **17** and **18**) are so poorly predictive (the Me_2NLi model could be at fault), the potential importance of the fluoro moiety to stabilize ring-expanded (open) dimers resurfaces (vide infra).

The nearly equal binding energies of *n*-BuOMe and DME in the reactant and 90-fold acceleration of the rearrangement suggest that DME is chelated in the transition state illustrated in eq 16. Such "hemilability" of DME-solvated LDA has been documented on several occasions.[38] Computations show a significant preference for the chelated form with affiliated ring expansion, as illustrated in eq 18. (Recall that caution is warranted here).

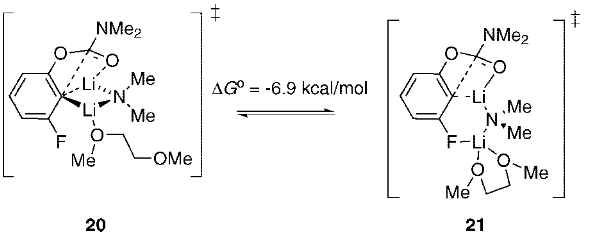

(18)

TMEDA and Me₂NEt. TMEDA surprisingly affords both mixed dimer **7g** and mixed trimer **8a**. We believed that chelation would disfavor trimers. Is TMEDA failing to chelate? Possibly. Me_2NEt, a nonchelating analog of TMEDA, also affords mixed dimer and trimer (**7h** and **8b**). Fries rearrangement of the mixed dimers and trimers in TMEDA and Me_2NEt with excess LDA yield trimers **10d** and **10e**. Rate studies using mixtures of starting materials are generally ill advised and were not pursued.

TMCDA. To study the role of a chelating diamine on the reaction rate and mechanism, we investigated TMCDA as a strongly coordinating model of TMEDA. Metalation of **4b** with LDA/TMCDA affords only aryllithium monomer **6g** even with excess LDA. This substantial change in structure, when compared with the results using TMEDA, suggests that TMCDA chelates and TMEDA does not. Monomer **6g** displays a characteristic ^{6}Li singlet and ^{13}C triplet. We were not, however, able to observe free and bound TMCDA using ^{13}C NMR spectroscopy. DFT calculations using, ironically, TMEDA as a

---

[37] See ref 10c and references therein.

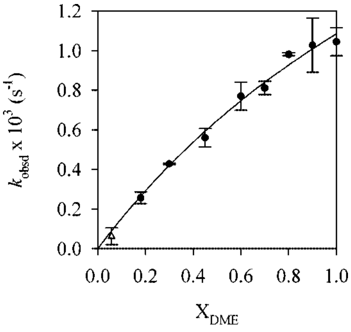

Figure 6. Plot of k_{obsd} vs mole fraction of DME (X_{DME}) for the rearrangement of **7e** (0.004 M) by LDA (0.05 M) at −60 °C. The donor solvent concentration is held constant ([DME] + [*n*-BuOMe] = 5.0 M) using pentane as cosolvent. The curve depicts an unweighted least-squares fit to $k_{obsd} = (a + bx)/(1 + cx)$ ($a = (0.0 \pm 0.1) \times 10^{-3}$, $b = 1.6 \pm 0.5$, $c = 0.5 \pm 0.4$) such that $1 + c = K_{eq}$ (see eq 17). At low DME concentrations the lithium phenolate precipitated during the reaction; the value of k_{obsd} (shown as △) was not included in the fit.

model for TMCDA suggest that the chelate is plausible. Rearrangement of **6g** at −25 °C affords a complex mixture of phenoxides. The complexity of the product distribution does not preclude detailed rate studies, however.

Plots of k_{obsd} vs TMCDA concentration and k_{obsd} vs LDA concentration for the rearrangement of monomer **6g** reveal zeroth-order dependencies. The idealized rate law in eq 19 is consistent with a single mechanism requiring no net changes in aggregation or solvation described generically in eq 20 and transition structure **22** (eq 2).[39]

$$-\mathrm{d}[\mathbf{6g}]/\mathrm{d}t = k'[\mathbf{6g}][\mathrm{TMCDA}]^0[\mathrm{LDA}]^0 \qquad (19)$$

$$\underset{(\mathbf{6g})}{(\mathrm{ArLi})(\mathrm{TMCDA})} \rightarrow \underset{(\mathbf{22})}{[(\mathrm{ArLi})(\mathrm{TMCDA})]^{\ddagger}} \qquad (20)$$

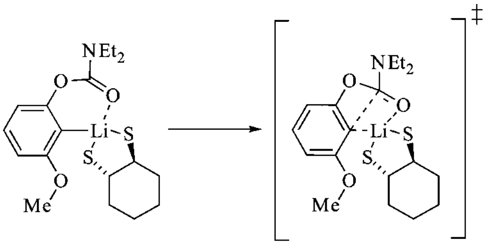

(21)

6g (S=NMe$_2$) **22** (S=NMe$_2$)

Discussion

We introduced the work described herein with solvent-dependent yields and rates of an archetypal Snieckus–Fries rearrangement shown in eq 1a. Noting that yields do not shed light on rates and simple relative rate constants do not shed light on causative organolithium structures and mechanisms, we embarked on studies of solvent-dependent structure–reactivity relationships. Control over both reactant structures and reaction rates—two important requisites of transparent mechanistic studies—demanded taking liberties in the choice of carbamoyl group and meta substituent. A coherent summary of the results, however, requires that we also take some linguistic liberties by largely ignoring the substrate variations and focusing on the influence of solvent. Scheme 2 summarizes these results. We do not wish to imply, however, that fluoro and methoxy moieties are interchangeable; substrate-dependent changes in mechanism may lurk undetected under the surface. The structures of the reactants assigned spectroscopically and the putative transition structures are supported by computations that are largely archived in Supporting Information.

Scheme 2

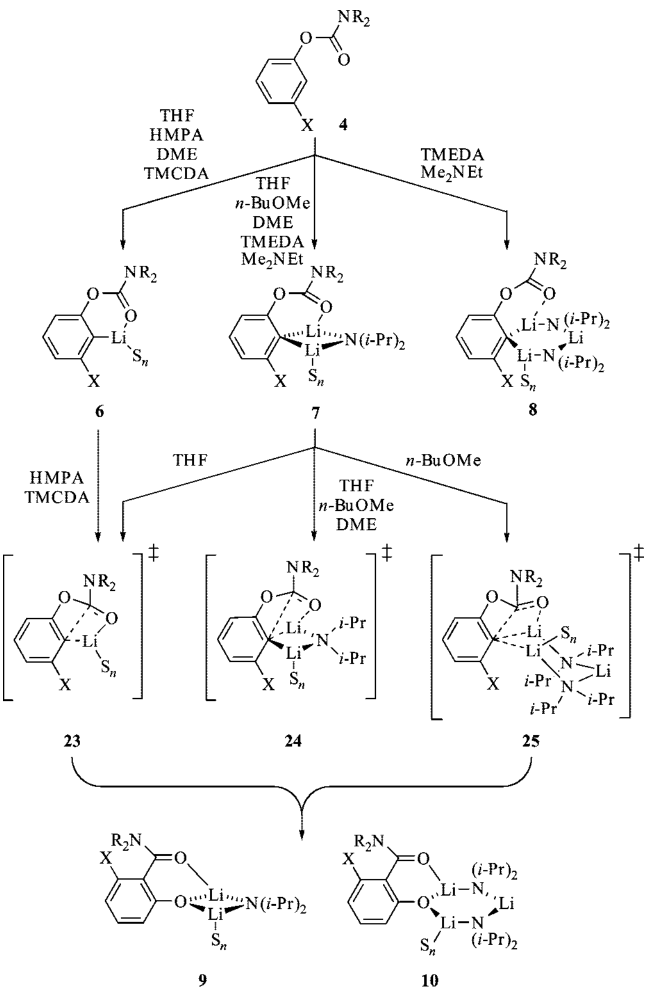

Solution Structures. The solvent-dependent structures of lithiated aryl carbamates follow fairly conventional patterns. The most strongly coordinating solvents such as TMCDA and HMPA promote monomers (**6**). The most strongly coordinating ethereal solvent (THF) can afford monomers, but affords mixed dimers (**7**) with excess LDA. The less strongly coordinating *n*-BuOMe promotes exclusively mixed dimers, whereas the very weakly coordinating Me$_2$NEt[10a,c,17c,40] affords mixtures of mixed dimers and mixed trimers. (Mixed trimers are generally favored by weakly coordinating solvents because of their relatively low per-lithium solvation numbers.)[7,17a,41,42] Previous studies, however, have shown that TMEDA is superior to DME as a chelating ligand.[43] By the simple paradigm that solvation energy correlates with aggregation state, therefore, DME appears to

---

[38] (a) Ramirez, A.; Collum, D. B. *J. Am. Chem. Soc.* **1999**, *121*, 11114. (b) Ramirez, A.; Lobkovsky, E.; Collum, D. B. *J. Am. Chem. Soc.* **2003**, *125*, 15376. (c) Remenar, J. F.; Collum, D. B. *J. Am. Chem. Soc.* **1997**, *119*, 5573.

[39] (a) We found that TMCDA prepared from commercially available *R,R*- and *S,S*-1,2-cyclohexanediamines did not afford equivalent rates of rearrangement. Although the source of the differences was not found, we alleviated the problem by resolving *trans*-cyclohexanediamine,[39b] N-methylating[17b] and recrystallizing the resulting TMCDA as its HCl salt.[17b] We found that the optical purity of *trans*-1,2-cyclohexanediamine and TMCDA could be evaluated by ^{13}C NMR spectroscopy by adding 2 equiv of (+)-taddol in toluene-d_8.[39c]. (b) Larrow, J. F.; Jacobsen, E. N. *Org. Synth.* **1998**, *10*, 96. (c) Seebach, D.; Beck, A. K.; Heckel, A. *Angew. Chem., Int. Ed.* **2001**, *40*, 92.

be a stronger ligand than TMEDA given that TMEDA affords mixed dimers and trimers. Indeed, tacit evidence suggests that TMEDA is too sterically demanding to chelate mixed dimer **7**, causing TMEDA to function equivalently to the poorly coordinating Me_2NEt.[44] On many occasions we have found that the often cited inverse correlation of solvent donicity (enthalpy of solvation) with aggregation number is flawed.[42] In this study, however, the old paradigm holds true.

Despite its complexity, the structure of the aryllithium was successfully controlled as monomer **6** (TMCDA and HMPA) or mixed dimer **7** (THF, *n*-BuOMe, and DME) as required for detailed rate studies.

Monomer-Based Reactivity. In the case of HMPA, solvation by an additional HMPA ligand occurs en route to the transition state. Two solvents eliciting the highest overall reaction rates (eq 1a) also foster monomer-based pathways; these results follow conventional wisdom. Previous studies had shown that THF-solvated mixed dimer **7** can rearrange either directly as the mixed dimer or via aryllithium monomer following deaggregation (see **12**). In this instance, the high rates observed at low LDA concentrations arise from the monomer-based rearrangement. Overall, as one might expect, the two solvents that afford observable monomers even in the presence of excess LDA also promote reaction via monomer-based transition structures.

Mixed Dimer-Based Reactivity. Mixed dimers are reactive forms for all of the ethereal solvents (although not exclusively so). The results in THF present an interesting mechanistic issue. A first-order THF dependence affiliated with the mixed dimer-based reaction suggests that a disolvated dimer-based pathway is operative (eq 4). Computations reveal that one of the reasonable transition structures has *an affiliated expanded ring resulting from chelation by the meta fluoro group*. This expanded ring is illustrated in transition structure **26**. We expressed some concern (vide supra) that the stability of such open dimers may be overstated, but we find them interesting.

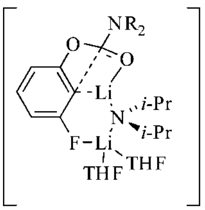

26

A similar effect shows up in rearrangements using DME. Binding studies show that DME and *n*-BuOMe are nearly equivalent ligands toward mixed dimer **7**, whereas *rate* studies show that the rearrangement is 90 times faster in DME (eq 1a). We infer, therefore, that DME is *not* chelated in the reactant but *is* chelated in the transition structure (eq 22). Marked rate accelerations stemming from the hemilability of DME are well documented for LDA-mediated metalations.[38] Computations suggest that the rearrangement proceeds via open dimer **27**. This role of the meta substituent once again provokes thought.

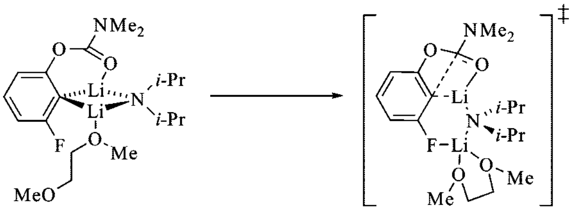

7e **27** (22)

Mixed Trimer-Based Reactivity. Metalations in *n*-BuOMe in which mixed dimer **7** is the observable reactant displayed an unusual (possibly unprecedented[11]) half-order LDA dependence affiliated with a nonzero intercept. The intercept signifies a pathway requiring no LDA dissociation from mixed dimer **7**, which implicates a mixed dimer-based pathway as discussed above. The half-order dependence, in conjunction with an inverse order *n*-BuOMe dependence, suggests a rearrangement mechanism requiring *an additional equivalent of LDA monomer*. The stoichiometry must be that of a mixed trimer, $[(i\text{-}Pr_2NLi)_2(ArLi)(n\text{-}BuOMe)]^{\ddagger}$[14] Of the >100 rate laws measured for LDA-mediated reactions to date,[11] we have not observed evidence of trimer- or mixed trimer-based reactivity. Moreover, we are unaware of any documented case of an organolithium reaction proceeding through a higher aggregation state than that observed for the reactants.[13] It is also interesting that simply changing from THF to *n*-BuOMe, arguably a fairly subtle change, causes the rearrangement to change from LDA inhibited to LDA promoted.

Conclusions

Studies of ortholithiated aryl carbamates show that changes in solvent afford marked shifts in structure from aryllithium monomer to LDA−aryllithium mixed dimers and trimers. The mechanisms of the subsequent Snieckus−Fries rearrangements underscore a similar structural diversity in the rate-limiting transition structures. In addition to the insights offered into the intimate interplay between solvent and substrate to control solution structure and reaction mechanism, one finds several surprising observations. The meta substituent on the aryl ring may play a role in the rearrangement beyond simply stabilizing the aryllithium that, given the importance of substituted aryllithiums in synthesis,[1,45] may be of significance. Also, an odd variant of hemilability[46]—the penchant for bifunctional ligands to accelerate organolithium reactions by chelating only in the rate-limiting transition state[38,47]—seems to have surfaced. As a final summarizing note, evidence that an observable mixed dimer undergoes further aggregation to mixed trimer, once again,

---

(40) (a) Lucht, B. L.; Collum, D. B. *J. Am. Chem. Soc.* **1996**, *118*, 2217. (b) Settle, F. A.; Haggerty, M.; Eastham, J. F. *J. Am. Chem. Soc.* **1964**, *86*, 2076. (c) Lewis, H. L.; Brown, T. L. *J. Am. Chem. Soc.* **1970**, *92*, 4664. (d) Brown, T. L.; Gerteis, R. L.; Rafus, D. A.; Ladd, J. A. *J. Am. Chem. Soc.* **1964**, *86*, 2135. (e) Quirk, R. P.; Kester, D. E. *J. Organomet. Chem.* **1977**, *127*, 111.

(41) Lucht, B. L.; Collum, D. B. *Acc. Chem. Res.* **1999**, *32*, 1035.

(42) Sun, X.; Collum, D. B. *J. Am. Chem. Soc.* **2000**, *122*, 2459.

(43) Lucht, B. L.; Bernstein, M. P.; Remenar, J. F.; Collum, D. B. *J. Am. Chem. Soc.* **1996**, *118*, 10707.

(44) (a) Bauer, W.; Klusener, P. A. A.; Harder, S.; Kanters, J. A.; Duisenberg, A. J. M.; Brandsma, L.; Schleyer, P. v. R. *Organometallics* **1988**, *7*, 552. (b) Köster, H.; Thoennes, D.; Weiss, E. *J. Organomet. Chem.* **1978**, *160*, 1. (c) Teclé, B.; Ilsley, W. H.; Oliver, J. P. *Organometallics* **1982**, *1*, 875. (d) Harder, S.; Boersma, J.; Brandsma, L.; Kanters, J. A. *J. Organomet. Chem.* **1988**, *339*, 7. (e) Sekiguchi, A.; Tanaka, M. *J. Am. Chem. Soc.* **2003**, *125*, 12684. (f) Linnert, M.; Bruhn, C.; Ruffer, T.; Schmidt, H.; Steinborn, D. *Organometallics* **2004**, *23*, 3668. (g) Fraenkel, G.; Stier, M. *Prepr. Am. Chem. Soc., Div. Pet. Chem.* **1985**, *30*, 586. (h) Ball, S. C.; Cragg-Hine, I.; Davidson, M. G.; Davies, R. P.; Lopez-Solera, M. I.; Raithby, P. R.; Reed, D.; Snaith, R.; Vogl, E. M. *J. Chem. Soc., Chem. Commun.* **1995**, 2147. (i) Wehman, E.; Jastrzebski, J. T. B. H.; Ernsting, J.-M.; Grove, J. M.; van Koten, G. *J. Organomet. Chem.* **1988**, *353*, 145. (j) Becker, J.; Grimme, S.; Fröhlich, R.; Hoppe, D. *Angew. Chem., Int. Ed.* **2007**, *46*, 1645. (k) Also, see ref 17c.

suggests that the correlation of aggregation state and reactivity requires some care. Thus, one is reminded that relationships among product yields, reaction rates, aggregate structures, and reaction mechanisms are often quite complex.

Experimental Section

Reagents and Solvents. THF, *n*-BuOMe, DME, Me_2NEt, hexane, toluene, and pentane were distilled from blue or purple solutions containing sodium benzophenone ketyl. The hydrocarbon stills contained 1% tetraglyme to dissolve the ketyl. HMPA was dried over CaH_2 and vacuum distilled. TMEDA and TMCDA were recrystallized as their HCl salts[39,48] and distilled from blue or purple solutions containing sodium benzophenone ketyl. Owing to evidence that commercially available *R,R*- and *S,S*-cyclohexanediamine may contain impurities that influence reaction rates, we resolved racemic *trans*-1,2-cyclohexanediamine following literature procedures.[39] LDA, $[^6Li]$LDA, and $[^6Li,^{15}N]$LDA were prepared from *n*-BuLi and *i*-Pr_2NH and recrystallized.[15] Air- and moisture-sensitive materials were manipulated under argon or nitrogen using standard glovebox, vacuum line, and syringe techniques. Solutions of *n*-BuLi and LDA were titrated using a literature method.[49] Aryl carbamates **4a**–**e** were prepared by literature procedures.[18]

NMR Spectroscopic Analyses. Standard ^1H and ^{13}C NMR spectra were recorded on a 300 MHz spectrometer. ^1H, ^6Li, ^{13}C, and ^{15}N NMR spectra were recorded on a 400, 500, or 600 MHz spectrometers. The ^6Li and ^{15}N resonances are referenced to 0.30 M $[^6Li]LiCl/MeOH$ at −90 °C (0.0 ppm) and neat Me_2NEt at −90 °C (25.7 ppm), respectively. The ^{13}C resonances are referenced to the CH_2O resonance of THF at −90 °C (67.6 ppm), the ipso resonance of toluene at 137.9 ppm, and methyl resonance of pentane at 14.1 ppm.

IR Spectroscopic Analyses. Spectra were recorded using an in situ IR spectrometer fitted with a 30-bounce, silicon-tipped probe. The spectra were acquired in 16 scans at a gain of 1 and a resolution of 8 cm^{-1}. A representative reaction was carried out as follows: The IR probe was inserted through a nylon adapter and O-ring seal into an oven-dried, cylindrical flask fitted with a magnetic stir bar and a T-joint. The T-joint was capped by a septum for injections and a nitrogen line. Following evacuation under a full vacuum, heating, and flushing with nitrogen, the flask was charged with LDA (25–500 mg) in a solvent/cosolvent solution (9.9 mL) and cooled in a temperature-controlled bath. After recording a background spectrum, a carbamate was added to the LDA/solvent/cosolvent mixture from a dilute stock solution (100 μL, 0.400 M) with stirring. IR spectra were recorded over the course of the reaction. To account for mixing and temperature equilibration, spectra recorded in the first 1.5 min were discarded. All reactions were monitored to >5 half-lives.

Acknowledgment. We thank the National Institutes of Health (GM 39764) and the National Science Foundation for direct support of this work and Merck, Pfizer, Boehringer-Ingelheim, R. W. Johnson, sanofi-aventis, Schering-Plough, and DuPont Pharmaceuticals (Bristol-Myers Squibb) for indirect support. We also thank Emil Lobkovsky for help with a crystal structure determination.

Supporting Information Available: NMR, rate, and computational data; complete reference 33. This material is available free of charge via the Internet at http://pubs.acs.org.

JA804087R

---

(45) (a) Gribble, G. W. In *Science of Synthesis*; Georg Thieme Verlag: New York, 2005; Vol. 8.1.14. (b) Clayden, J. *Organolithiums: Selectivity for Synthesis*; Pergamon: New York, 2002. (c) Schlosser, M. In *Organometallics in Synthesis: A Manual*, 2nd ed.; Schlosser, M., Ed.; John Wiley: Chichester, 2002; Chapter 1. (d) Clayden, J. In *The Chemistry of Organolithium Compounds*; Rappoport, Z., Marek, I., Eds.; Wiley: New York, 2004; Vol. 1, p 495.

(46) For reviews of hemilabile ligands, see: (a) Braunstein, P.; Naud, F. *Angew. Chem., Int. Ed.* **2001**, *40*, 680. (b) Slone, C. S.; Weinberger, D. A.; Mirkin, C. A. *Prog. Inorg. Chem.* **1999**, *48*, 233. (c) Lindner, E.; Pautz, S.; Haustein, M. *Coord. Chem. Rev.* **1996**, *155*, 145. (d) Bader, A.; Lindner, E. *Coord. Chem. Rev.* **1991**, *108*, 27.

(47) (a) Ramirez, A.; Sun, X.; Collum, D. B. *J. Am. Chem. Soc.* **2006**, *128*, 10326. (b) Liou, L. R.; McNeil, A. J.; Ramirez, A.; Toombes, G. E. S.; Gruver, J. M.; Collum, D. B. *J. Am. Chem. Soc.* **2008**, *130*, 4859.

(48) (a) Rennels, R. A.; Maliakal, A.; Collum, D. B. *J. Am. Chem. Soc.* **1998**, *120*, 421. (b) Freund, M.; Michaels, H. *Ber.* **1897**, *30*, 1374.

(49) Kofron, W. G.; Baclawski, L. M. *J. Org. Chem.* **1976**, *41*, 1879.